# AVERAGE THERMAL CHARACTERISTICS OF SOLAR WIND ELECTRONS

*Michael D. Montgomery*

ABSTRACT This contribution presents average solar wind electron properties based on a 1 year Vela 4 data sample—from May 1967 to May 1968. Frequency distributions of electron-to-ion temperature ratio, electron thermal anisotropy, and thermal energy flux are presented. The resulting evidence concerning heat transport in the solar wind is discussed.

## INTRODUCTION

As is well known, the information concerning electrons in the solar wind published to date is quite fragmentary [*Wolfe and McKibbin* 1968; *Serbu*, 1968; *Montgomery et al.*, 1968; *Ogilvie et al.*, 1971]. Here we present some average solar wind electron properties based on a more extended and significant Vela 4 data sample. The sample to be used covers the year from May 1967 to May 1968. We concentrate on the thermal properties of the electron component of the plasma, in particular, the electron-to-ion temperature ratio, the electron thermal anisotropy, the total pressure anisotropy, and thermal conduction properties.

## ELECTRON-TO-ION TEMPERATURE RATIO

Figure 1 contrasts the proton and electron temperature variation with solar wind speed. Approximately 6000 temperature measurements from the one-year interval defined above are divided into 100 km/sec speed intervals. The averages within each interval are plotted versus solar wind speed. The proton temperature-velocity relationship is essentially the same as has already been published [*Burlaga and Ogilvie*, 1970; *Hundhausen et al.*, 1970]. In contrast, the electron temperature is almost constant but there is a possible slight increase with velocity. This rise may be due to a small amount of electron heating associated with the interaction region between high- and low-velocity streams [*Burlaga et al.*, 1971; *Hundhausen and*

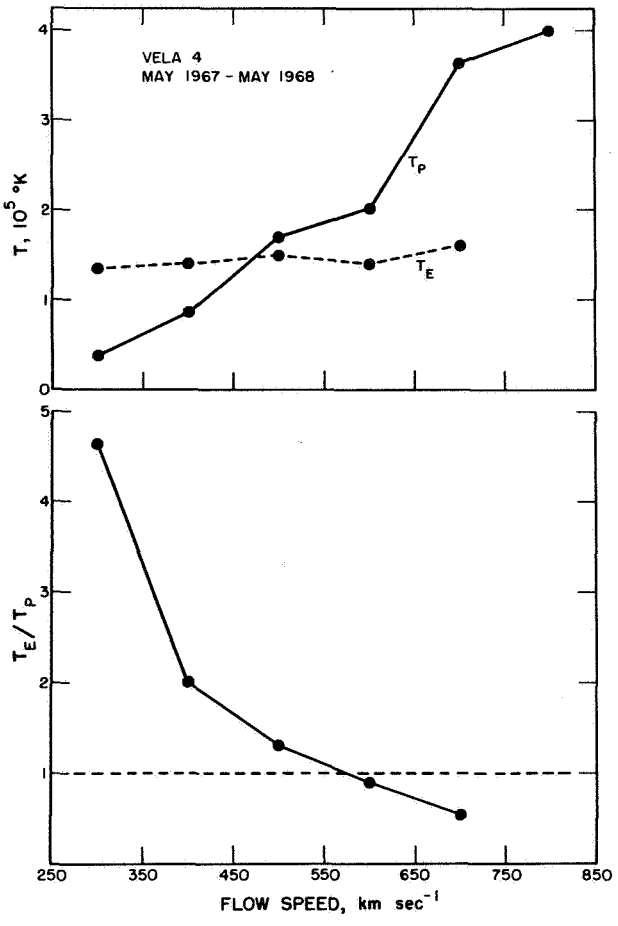


**Figure 1.** *Variation of electron and proton temperature with flow speed. Each point represents an average over a 100 km $sec^{-1}$ interval.*

*The author is at the University of California, Los Alamos Scientific Laboratory, Los Alamos, New Mexico.*

*Montgomery*, 1971]. The electron-to-proton temperature ratio is plotted in the the lower panel of figure 1. During quiet times (low solar wind speeds) an electron-to-ion temperature ratio of about 4 is a good average. However, since most of the measurements are situated at about 400 km/sec, the overall average temperature ratio is about 2. The fact that the electron temperature in the solar wind is much more constant than the proton temperature can be explained by the relatively high thermal conductivity of the electrons [*Hundhausen and Montgomery*, 1971].

## ELECTRON THERMAL ANISOTROPY

Figure 2 shows the Vela 4 proton thermal anisotropy distribution. This distribution differs little from that of Vela 3 [*Hundhausen et al.*, 1970]. The Vela 4 average of 1.5 is somewhat smaller than the average of 1.9 from Vela 3, but it must be understood that what is measured is the projection of the temperature ratio onto the plane of analysis [*Hundhausen et al.*, 1967; *Montgomery et al.*, 1970]. Thus, the fact that the spin axis of Vela 4 was always pointed away from earth along a radius vector while that of Vela 3 was nearly perpendicular to the ecliptic plane may account for the smaller average Vela 4 value. The histogram showing the distribution of electron temperature anisotropy measured by Vela 4 is presented by figure 3. It can be easily seen that the average is *much smaller* than for protons–about 1.1. If one takes into account the projection on the analysis plane, the true value could be as high as 1.2.

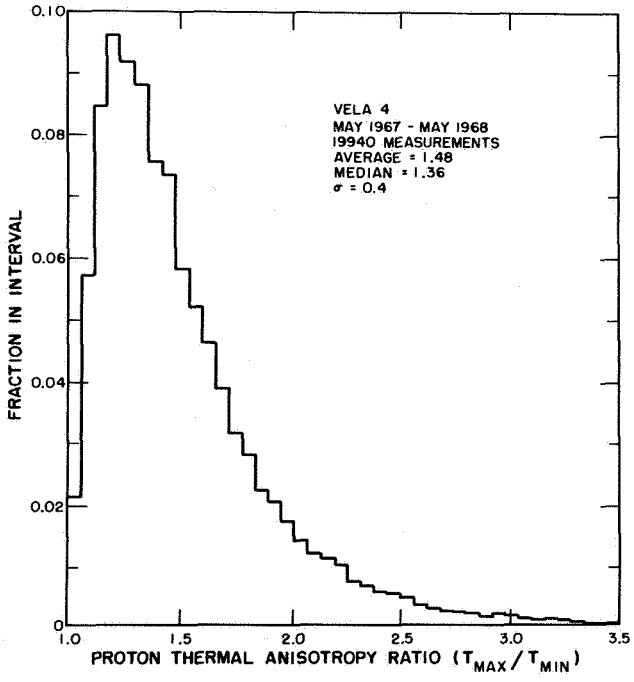


**Figure 2.** *Distribution of proton thermal anisotropy. 90 percent of the values are < 2.0.*

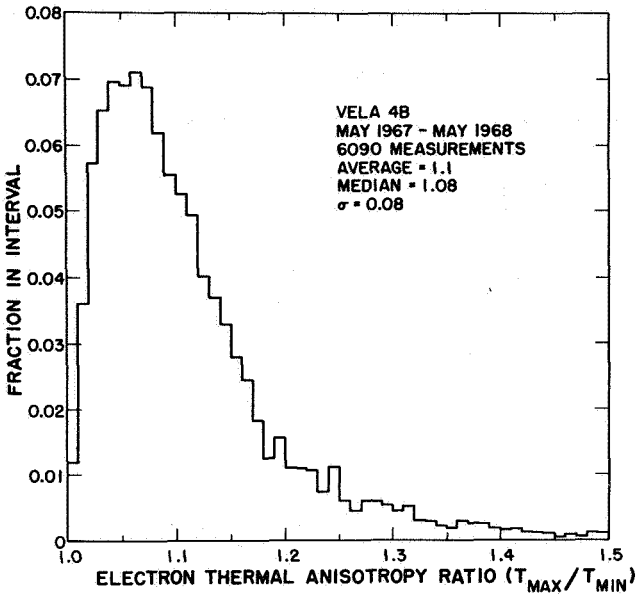


**Figure 3.** *Distribution of electron thermal anisotropy. 90 percent of the values are < 1.22.*

## TOTAL PRESSURE ANISOTROPY

For those interested in doing magnetohydrodynamic calculations, the total pressure anisotropy is of major interest. The total pressure anisotropy distribution is given by figure 4. The average is about 1.2; but due to projection, it could be as high as, but probably less than, 1.4. Thus, for most purposes, thermal anisotropies are relatively unimportant in the solar wind.

## THERMAL CONDUCTION

The Vela results concerning thermal conduction are summarized in figure 5. This figure simply shows the measured thermal energy flux distribution where, again, the measured values are really projections onto the spacecraft equatorial plane. The effect of the projection is probably less than about $\sqrt{2}$; that is, the true magnitudes of the energy flux are probably about $\sqrt{2}$ times greater than indicated. It should be noted that the average value given here of $\sim 7 \times 10^{-3}$ erg cm$^{-2}$ sec$^{-1}$ turns out to be less than that given by early samples of Vela 4 data [*Montgomery et al.*, 1968] where a range of 0.005-0.02 erg cm$^{-2}$ sec$^{-1}$ was quoted. It is instructive to compare the measured thermal energy flux with what one would expect assuming completely collision

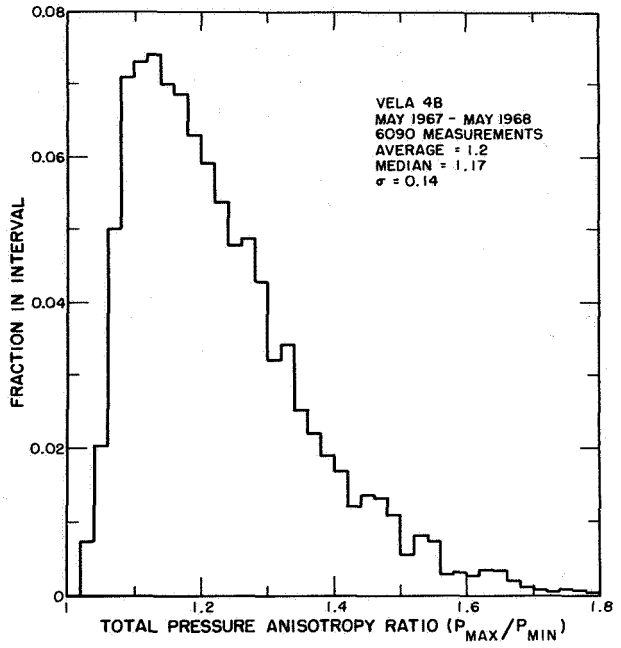


**Figure 4.** *Distribution of total pressure anisotropy. 90 percent of the values are < 1.42.*

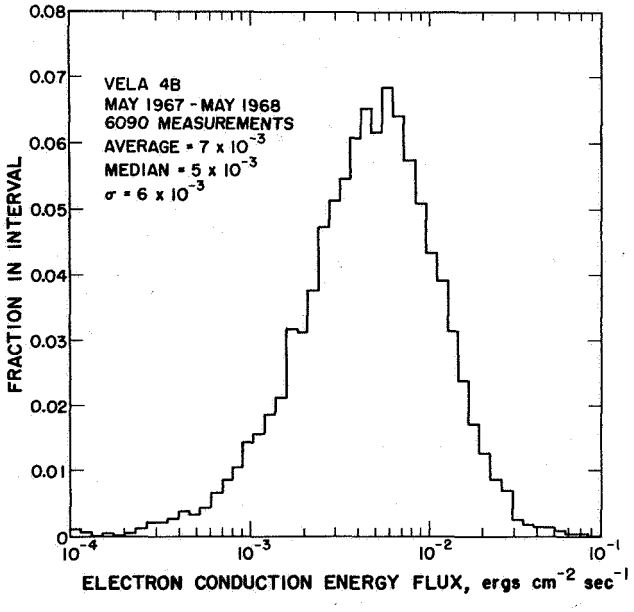


**Figure 5.** *Distribution of electron heat conduction flux density.*

dominated classical thermal conductivity [*Spitzer and Härm,* 1953; *Forslund,* 1970]. This comparison can be carried out with the aid of a dimensionless parameter $B_T$ that was used as an expansion parameter in the Spitzer-Härm theory. The Spitzer-Härm approximation is expected to be valid only for $B_T \ll 1$ [*Forslund,* 1970]. The parameter $B_T$ can be defined in two equivalent ways:

$$B_T \equiv \lambda_{mfp} / \lambda_{\nabla T} \tag{1}$$

or

$$B_T \equiv E_F / E_{F(sat)} \tag{2}$$

where $\lambda_{mfp}$ is the electron-electron collision mean free path, $\lambda_{\nabla T}$ is the scale length of the thermal gradient in the solar wind $(dT/T\,dr)^{-1}$, $E_F$ is the measured energy flux, and $E_{F(sat)}$ is the saturation energy flux defined as the energy flux obtained if the internal energy of the electrons is transported at the electron thermal speed [*Parker,* 1964]. For this study a conduction-dominated radial temperature dependence of $T = T_0(r/r_0)^{-2/7}$ and a magnetic field direction of 45° from radial were assumed. Under these assumptions, (1) can be rewritten as

$$B_{T2} = 1.8 \times 10^{-10} T_E^{\,2} / n \tag{3}$$

where $T_E$ is electron temperature (°K) and $n$ is particle density in $cm^{-3}$, and (2) can be rewritten

$$B_{T1} = E_F / V_{th}(3/2) n k T_E \tag{4}$$

where $V_{th}$ is the electron thermal speed. Both $B_T$ can be evaluated by measuring $T_E$, $n$, and $E_F$, and then compared. The results are shown in figure 6 where the dashed histogram represents the distribution of $B_{T2}$

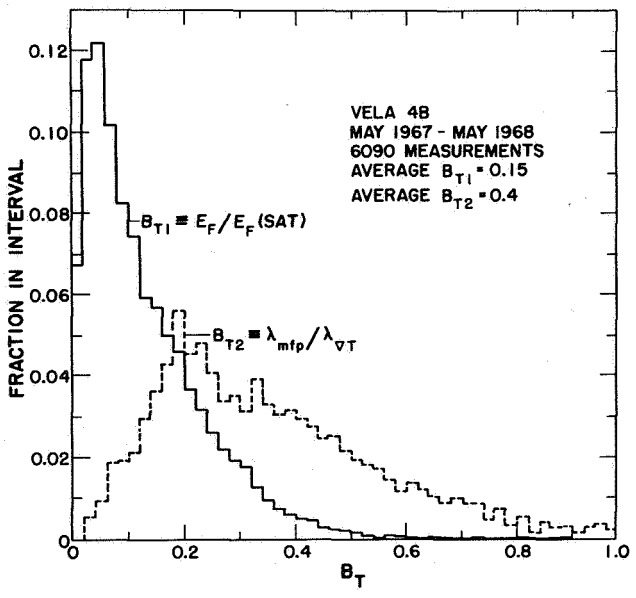


**Figure 6.** *Comparison of experimental ($B_{T1}$) and theoretical ($B_{T2}$) heat flux parameters. See the text for definitions and discussion.*

evaluated from (3) while the solid histogram represents $B_{T1}$ evaluated from (4). It is important to note that there is a significant difference in the average values of $B_{T1}$ and $B_{T2}$. In fact, they differ by about a factor of 3. A likely conclusion is that use of the collision-dominated conductivity is probably not valid, and a quasi-collisionless kind of conductivity should be substituted. Other papers in this chapter include some discussion on this point; see Comments by Perkins (p. 215). In addition, since large $B_T$ implies a large skewing of the electron velocity distribution, it is possible that plasma instabilities may contribute to the reduction of the thermal conductivity [*Forslund,* 1970].

## SUMMARY

A representative one-year sample of Vela 4 solar wind data gives the following results:

1. $T_E$ is much less variable than $T_P$.
2. Thermal anisotropies are much smaller for electrons than for protons.
3. The total pressure anisotropy in the solar wind is small and relatively unimportant for many purposes.
4. The measured thermal energy flux in the solar wind is much smaller than expected on the basis of a collision dominated thermal conductivity. Thus, the actual thermal conductivity of the solar wind is probably significantly less than the classical value. This reduction in conductivity may be due to heat-conduction-generated plasma instabilities.

## ACKNOWLEDGMENTS

The Vela nuclear test detection satellites have been designed, developed, and flown as a part of a joint program of the Advanced Research Projects Agency of the U.S. Department of Defense and the U.S. Atomic Energy Commission. The program is managed by the U.S. Air Force.

## REFERENCES

Burlaga, L. F.; and Ogilvie, K. W.: Heating of the Solar Wind. *Astrophys. J.*, Vol. 159, 1970, p. 659.

Burlaga, L. F.; Ogilvie, K. W.; Fairfield, D. H.; Montgomery, M. D.; and Bame, S. J.: Energy Transfer at Colliding Streams in the Solar Wind. *Astrophys. J.*, Vol. 164, 1971, p. 137.

Forslund, D. W.: Instabilities Associated with Heat Conduction in the Solar Wind and Their Consequences. *J. Geophys. Res.*, Vol. 75, 1970, p. 17.

Hundhausen, A. J.; and Montgomery, M. D.: Heat Conduction and Nonsteady Phenomena in the Solar Wind. *J. Geophys. Res.*, Vol. 76, 1971, p. 2236.

Hundhausen, A. J.; Asbridge, J. R.; Bame, S. J.; Gilbert, H. E.; and Strong, I. B.: Vela 3 Satellite Observations of Solar Wind Ions: A Preliminary Report. *J. Geophys. Res.*, Vol. 72, 1967, p. 87.

Hundhausen A. J.; Bame, S. J.; Asbridge, J. R.; and Sydoriak, S. J.: Solar Wind Proton Properties: Vela 3 Observations from July 1965 to June 1967. *J. Geophys. Res.*, Vol. 75, 1970, p. 4643.

Montgomery, M. D.; Bame, S. J.; and Hundhausen, A. J.: Solar Wind Electrons: Vela 4 Measurements. *J. Geophys. Res.*, Vol. 73, 1968, p. 4999.

Montgomery, M. D.; Asbridge, J. R.; and Bame, S. J.: Vela 4 Plasma Observations Near the Earth's Bow Shock. *J. Geophys. Res.*, Vol. 75, 1970, p. 1217.

Ogilvie, K. W.; Scudder, J. D.; and Sugiura, M.: Electron Energy Flux in the Solar Wind, submitted to *J. Geophys. Res.*, 1971.

Parker, E. N.: Dynamical Properties of Stellar Coronas and Stellar Winds, 2, Integration of the Heat Flow Equation. *Astrophys. J.*, Vol. 139, 1964, p. 93.

Serbu, G. P.: Low-Energy Plasma Measurements Obtained in Lunar Orbit. *Trans. Amer. Geophys. Union,* Vol. 49, 1968, p. 234.

Spitzer, L., Jr.; and Härm, R.: Transport Phenomena in a Completely Ionized Gas. *Phys. Rev.*, Vol. 89, 1953, p. 977.

Wolfe, J. H.; and McKibbin, D. D.: Pioneer 6 Observations of a Steady-State Magnetosheath. *Planet Space Sci.*, Vol. 16, 1968, p. 953.

## COMMENTS

*J. D. Scudder* The variability of interplanetary magnetic field from its average spiral configuration is exploited in this analysis of data from the OGO-E electron spectrometer to determine the energy flux transport in the rest frame of the plasma in the solar wind. We have proceeded on the hypothesis that the velocity distribution is axially symmetric about the magnetic field direction and roughly time independent on a time scale of several hours, as you have seen indicated in Montgomery's data. The rough time independence of the velocity distribution essentially implies that it is constant in shape when described about the magnetic field direction. Under this hypothesis we have determined the magnitude of the energy transport vector per unit solid angle, which we

call $Q_\Omega$, by computing the third moment of the empirical distribution function. Because of time limitations I will not show you exactly why you would expect this to be non-zero, but you've probably seen it in the literature. The asymmetry of the velocity distribution essentially gives rise to this non-zero character.

Figure 1 is a schematic idealization of what one might expect for energy transport per unit solid angle. If the energy flow were isotropic and one plotted the magnitude of $Q_\Omega$ versus $\beta$, which is the angle the transport direction would make with the magnetic field line, one would get essentially an isotropic picture as indicated in the top panel; if there were some preferred direction for the flow with respect to the field one would see something like the right-hand side of the middle panel; if the preferred direction were that of the magnetic field, one would either see something like the lower panel of this figure or its mirror image in the line $\beta = \pi/2$ if the interplanetary magnetic field polarity were reversed.

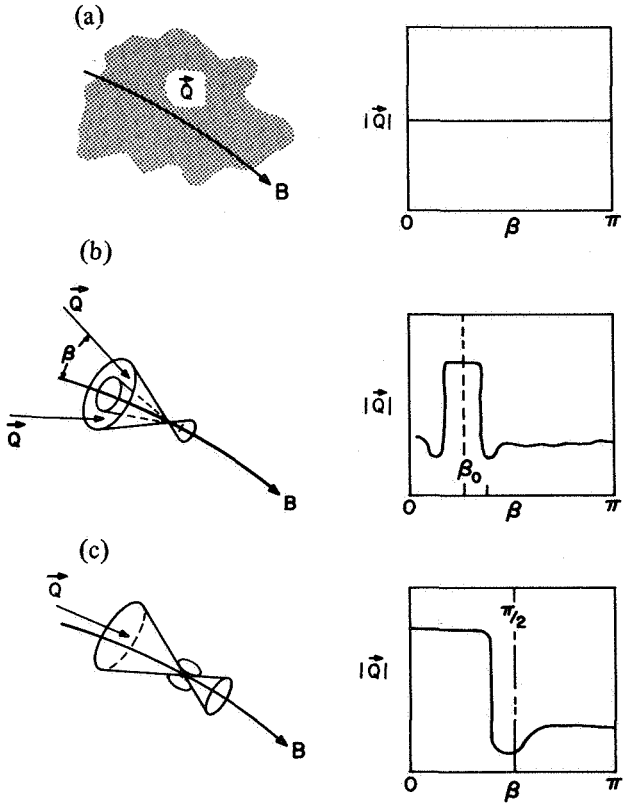


**Figure 1.** *Schematic representation of energy flux density $\langle Q_\Omega(\beta)\rangle$ versus $\beta$ for various physical situations; (a) energy flux uncorrelated with field direction; (b) correlation with empty cone about field; (c) energy flux filling cone about field line.*

If one assembles the data in this manner we see typically something which looks like the lower two panels. Two examples of our data have been plotted in figure 2 with only worst error bars indicated. If the data points don't have error bars on them the errors are too small to show. What one can see in this figure is that the flow direction for the flux is basically outward from the sun, regardless of sector polarity and is controlled by the field direction for a selected time interval when there is a good idea there is *no* bow shock intersection (from the vector magnetic field on the same spacecraft). The rather

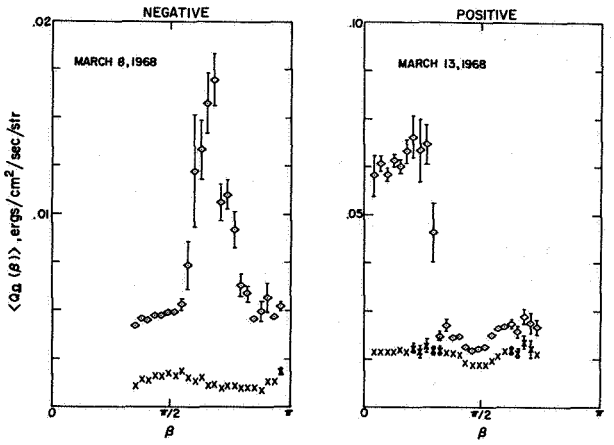


**Figure 2.** *Plots of $\langle Q_\Omega(\beta)\rangle$, the differential contributions to the energy flux density per unit solid angle, for angular intervals of 5°. Note that β is the angle between* **v** *and* **B**. *Sector polarity as indicated. Diamonds imply $E_u$ = 9.9 keV; crosses, $E_u$ = 0.340 keV.*

well-defined cone of energy flux transport per unit solid angle at $\beta$ less than 50° and the approximate flatness of the step for the positive sector example indicates a uniform population in this cone. The relative minima at $\pi/2$ suggest some inhibition of energy transport in the transverse direction. A similar example for a negative sector also shows outward flow as well as field control much like the middle panel of figure 1.

On a shorter time scale we can see the same type of phenomena, in figure 3, where we have plotted for the three mutually orthogonal detectors of our spectrometer system the magnitude of $Q_\Omega$ as computed from each one of them. The point to keep in mind here is that this data is for a time period determined as an outward sector; therefore, if the flux transport is along the magnetic field line (if $\beta$ is small) as in the top detector, the

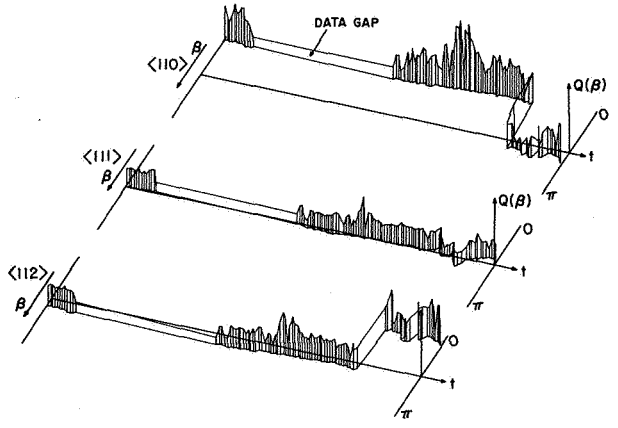


**Figure 3.** *Isometric plots for each detector showing that the largest flux is detected by that detector "looking" closest to the magnetic field line, and that this condition is preserved as the magnetic field direction shifts with respect to the triad of directions of the detectors. This is interpreted as showing that the energy flux is greatest along the field direction away from the sun.*

amplitude of $Q_\Omega$ should be large, as it is. If $\beta \gtrsim \pi/2$ the magnitude of $Q_\Omega$ is rather small, as it is monitored by detector (111) and, you can see in detector (112) that if the field is shifting from the transverse direction into the forward cone the amplitude of $Q_\Omega$ the energy flux transport per unit solid angle is increasing as it comes into the forward cone. We have concluded on the basis of this and other examples that the axis of the $Q_\Omega$ cone (i.e., the energy flux transport cone) is that of the *vectorial* field line, so that on average the *net* energy transport is away from the sun regardless of the sector designation when not on field lines intersecting the shock.

Previous measurements by Montgomery and Ness have shown that $\mathbf{Q}_\Omega$ is parallel to the projection of $B$ into the plane of their analysis. The result here is basically an extension of their result, using the entire vectorial magnetic field.

The magnitude of the *net* energy flux transport in the plasma frame is just the projection of this vector onto the magnetic field. It is important to note that $Q_\Omega$ as shown here is an integral over a finite interval of the velocity distribution function. Therefore, it is implicitly a function of the uppermost energy included in the distribution function itself.

In the lower panel of figure 4 we present several curves of $E$ parallel, that is, the net energy transport in the rest frame of the plasma, versus the upper energy involved in the empirical distribution function. The spectrometer on OGO-5 assembled the velocity distribution function from 10 eV to 10 kV. The curves shown here are for three successive passages in the interplanetary medium near apogee where field line intersection with the bow shock was highly improbable. The important things here are the two domains apparent in these examples. The convergent region of $E_\parallel (E_u)$, $E_u \sim 210$–$340$ eV, and the divergent contributions to $E_\parallel$ above this point. Although $E_\parallel (E_u)$, $E_u \gtrsim 340$, shows increasing divergences for the three examples $E_{||} (E_u), E_u < 300$ eV, remains relatively insensitive to the modified form of the distribution at higher energies which causes the divergence. We understand this temporal variability of $E_\parallel$ as being caused by particles associated with a delayed type solar electron event, as has been discussed in the literature by Lin and Anderson. You can see plotted on the top of this same figure the integral electron fluxes above 22 kV and above 45 kV, respectively, from Lin's particle counters on Explorer 35 orbiting the moon. The day when our $E$ parallel vs. $E_u$ curve is least divergent corresponds to the point (A) in Lin's fluxes where the integral fluxes above 22 kV are essentially at the quiet background that they have been at for some several days previous. On day 71, when we start to see an increasingly divergent behavior indicating particle populations down as low as 1 kV being influenced we see a thirtyfold enhancement (at point B) of Lin and Anderson type particles between 22 and 45 kV. If we take the spectra that we have on day 71, and we take information that Bob Lin was able to supply us on the spectral index between 25 and 45 kV and piece together the velocity distribution function within the errors of absolute intercalibration, the velocity distributions fit together very nicely. Thus we have an example of the solar wind plasma velocity distribution function merging with some type of transient phenomena.

Also of interest is an experimental value for $H_\parallel$ predicted by solar wind theories as the heat conduction under quiet solar wind expansion. Among other things, these theories assume a spherically symmetric corona and do not take into account transient energy flow injections. Therefore, it should not be too hard to swallow the idea that $H_\parallel$, the heat conduction, as a component of the overall energy flow in the plasma rest frame, should be less than any quantity plotted here. We have identified the value of $E_\parallel$ in the convergence zone to be the quantity most directly associated with the quiet time heat flux, $H_\parallel$. Then $H_\parallel \lesssim 4 \times 10^{-3}$ erg/cm$^3$ even during the height of the high energy solar particle fluxes. An absolute upper ground for a very conservative estimate would be $E_\parallel$ (10 keV) on day $68 \sim 1.6 \times 10^{-2}$. These examples are from cases when the magnetic field line does not intersect the bow shock with a high probability. The results that Mike

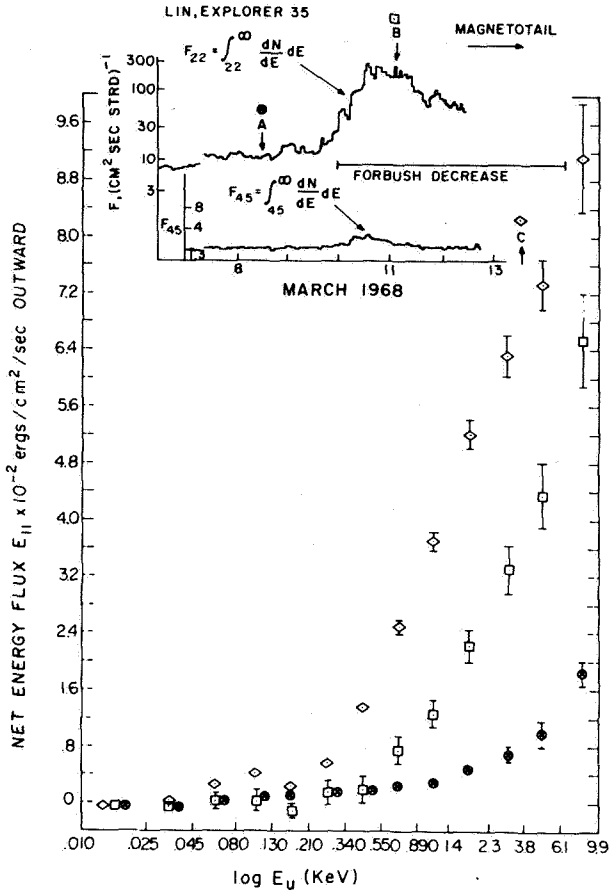


**Figure 4.** *$E_{\|}$ as a function of log $E_u$ for three periods during a "delayed" electron event (Lin and Anderson, private communication). The circles (pt. A in the inset) refer to a time of low solar electron flux, the squares and diamonds (pt. B, C in the inset) refer to a time of higher solar electron flux. The event is discussed further in the text. Note how extrapolating back to $E_{\|} = 0$ on all three curves crosses the axis between 210–340 eV.*

Montgomery has just presented are certainly consistent with this bound. Thus, in addition to our directional conclusions of $E_{\|}$ and also its transient behavior on a scale of several days, this determination shows that $H_{\|}$ is in fact small; it is small even in the sure absence of bow shock contaminations.

**COMMENTS**

*F. W. Perkins* I would like to present some thoughts on how you go about calculating the electron heat conductivity in a collisionless plasma. First of all, in order to describe how to compute the heat conductivity, let's look at the collisionless motion of electrons in the solar wind. The electrons move essentially at constant energy under the influence of an electrostatic radial electric field which occurs in all ionized atmospheres and holds the electron in and at constant magnetic moment $\mu$. Therefore the parallel motion of the electrons occurs in sort of a potential well; the bulk of the electrons have an oscillatory motion in the solar wind, bouncing back and forth between an electrostatic reflection on the outside and a magnetic mirror on the inside. A few energetic electrons are sufficiently energetic to overcome the potential barrier and escape; but with the bulk of electrons there is an oscillatory motion with an amplitude of the order of the radial distance $r$

from the sun and a frequency which I call $\omega_b \sim V_{th_e}/r$, because it bounces back and forth, essentially given by the thermal speed divided by the radial distance $r$. The collisionless picture will apply provided this bounce frequency is bigger than the collision frequency.

Let's see how this is reflected in the electron velocity distribution. It is obvious from the last picture that for the bulk of the electrons they must have an essentially even distribution in $V_\parallel$. There will be a few escaping photoelectrons that override the potential. In the middle of this even distribution in $V_\parallel$ sit the solar wind ions separated by the solar wind velocity. So the ions see most of the electrons drifting backwards. Second, this backward drift is well known to cause a lot of plasma instabilities. This is the type of velocity distribution Forslund used in discussing plasma instabilities associated with thermal conduction. The point I would like to make here is that thermal conduction and temperature gradients aren't really necessary to produce this type of velocity distribution. It's a natural type of velocity distribution the solar wind electrons would get into if the collisions just stopped; and I think it's this type of velocity distribution that is equally important compared with the anisotropies in driving plasma wind instabilities.

Let's see how this all fits in with the heat conductivity $k$. Heat conductivity, like a diffusive process, is proportional to the square of the step size times the frequency at which this step size happens, and for the heat conductivity you have to put in the number density. But in the Spitzer conductivity the step size is essentially the thermal speed divided by the coulomb collision frequency. If this step size is longer than the average bounce motion, then the Spitzer conductivity does not apply. If you put the step size together with the coulomb collision frequency you get $k \propto T_e^{5/2}$ –the neoclassical conductivity. Neoclassical is a word that is creeping into plasma physics literature confusion, which means that you do the right collisionless orbits but you put in the strict coulomb binary collisions. It comes out this way. For the step size we use the radial distance from the sun. For the collision frequency we use the coulomb collision frequency and thus, the scaling properties of this collision frequency are $k \propto n^2 r^2 T_e^{-3/2}$. A neoclassical conductivity will really inhibit the heat flow as the density gets lower. But I said that the velocity distribution causes plasma instabilities. And you can estimate the collision frequency associated with those instabilities just by requiring that collision frequencies essentially match an order of magnitude of the time scale in which this velocity distribution is set up. Well, this velocity distribution is set up in essentially one electron bounce time, and so I think that $\omega_b$ is a good estimate for the collision frequency caused by instability. You use the same step size, you put in the bounce frequency, and this is what I would propose to use as a heat conductivity formula in the solar wind, and it scales like $k \propto nrT_e^{1/2}$.

Well, you can always put numbers in the conductivity formulas. If you do it for what I thought about before the talks was a reasonable value, you would get the Spitzer conductivity about a factor of 4 larger than the instability conductivity. You can also estimate the rate at which energy exchange must occur if you have a specific instability in mind. Here I have the ion-sound instability. It occurs at a much faster rate than it would from a coulomb collision of essentially the rate $V_{SW} r^{-1}$

**DISCUSSION** *J. V. Hollweg* I have a comment and a question. The comment is that the electron distribution that you drew compared to the ion distribution looks like it implies a radial current from the sun which would lead to a loss of charge from the sun and therefore can't exist.

The question is, do you calculate electron thermal anisotropies in your model?

*F. W. Perkins* The velocity distribution that I discussed was supposed to have zero net moment compared to the outward going velocity of the solar wind. There were a few high energy escaping photoelectrons precisely equal to the net outward flow of ions. I don't

compute anisotropies. I imagine they would be very small because the electrons are essentially stuck in the solar wind, and execute many bounce motions.

*J. V. Hollweg* On that latter point, this calculation has similarities to a model that Jockers did of an exospheric solar wind. He considered electrons executing bounces, but the bounces were not mirror bounces. Instead the motion was equilibrated with the maxwellian distribution at the source. He found electron thermal anisotropies of the order of 3 which is, of course, much larger than observed.

On your first point, may I ask how the ion sound instability is driven if there is no current. Is it by heat conduction?

*F. W. Perkins* The ion sound instability depends on the slope of the electron velocity distribution in the neighborhood of the ions. It has a positive slope for a backward going wave. This model definitely predicts that backward going waves are unstable. Since the solar wind is both supersonic and super-Alfvénic it also predicts an instability for backward going Alfvén waves. All of this was brought out in Forslund's paper. This is just another way of getting the velocity distribution–perhaps in a way that is more physically motivated.

*Unidentified Speaker* In the previous talk on the energy flux you excluded the cases where the magnetic field lines intersected the bow shock. Can you tell us what happens under those circumstances?

*J. D. Scudder* Figure (A) shows the data for $E_{\|}$ vs. $E_u$ for an example where bow shock intersection was extremely probable on March 19, 1968 when the bulk speed

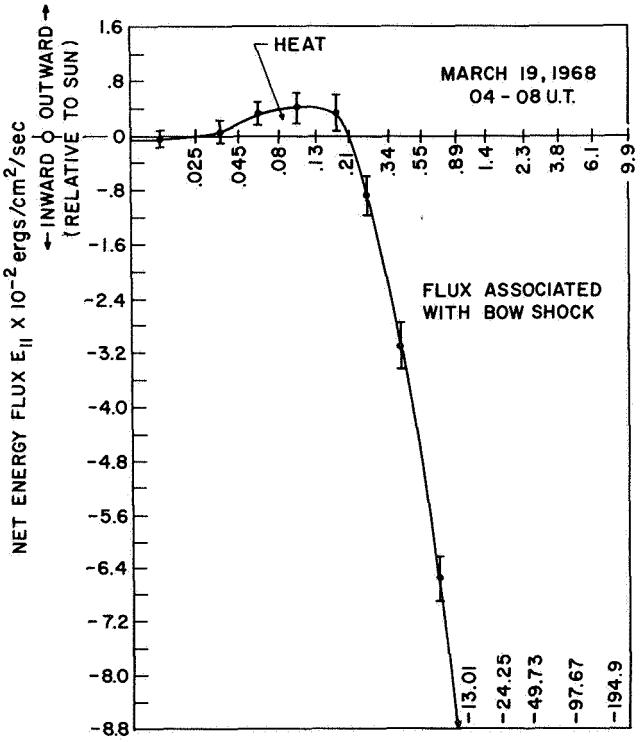


**Figure A.** *The net energy flux $E_{\|}$ plotted against log $E_u$, the uppermost energy to which it is calculated. Values of $E_{\|} > 0$ represent flux direction away from the sun, and values $< 0$ represent flux toward the sun (away from the earth's bow shock) along the magnetic field line. In this example the field almost certainly intersects the earth's bow shock.*

was ~600 km/sec. We note again the presence of two domains, the convergent and divergent zones. The net heat flux (i.e., $E_{\parallel}$ (~130 eV)) is outwardly directed, whereas the divergent higher energy contribution flow is *toward* the sun with extremely large net reverse flows which swamp the outward heat flux at lower energy. So you can see that the magnitude of this reverse transport is quite large; therefore, if there is significant flux coming back up field lines that interfere with velocity distribution calculations in the large, it can tend to reduce the asymmetry of the distribution function and therefore reduce the third moment.

*M. Dryer* I have a question for Mike Montgomery. You showed the temperatures of the protons and the electrons plotted versus the velocity, in which the former increased while the latter stayed fairly constant. Does this indicate that there is a preferential heating of the protons at discontinuities of various kinds?

*M. D. Montgomery* Not necessarily. I think the proper interpretation is that in most nonsteady phenomena in the solar wind, the source strength of local heating is not strong enough to saturate completely the local thermal conductivity. Therefore, the conductivity is enough to spread that heat over a large region and the temperature gradients are small in the electrons, but large in ions.

*F. C. Michel* How is the conductivity related to the heat flux? It seems unlikely that kilovolt electrons, which you (Montgomery) find to contribute most of the heat flux, are going to flow in response to thermal gradients that are the order of only a few electron volts. Such a heat flux may be intrinsic and not generated by thermal gradients.

*M. D. Montgomery* In our distributions, which we believe were taken on field lines that don't connect to the bow shock (we have eliminated such data from the sample), most of the heat flux is carried by the electrons of much smaller energy than that. Most of the energy is carried by electrons of the order of 50 to 100 eV. Now, why this is higher than a few eV I can't tell you.

*J. D. Scudder* The figures we have shown are certainly consistent with the major portion of the heat flux coming from energies below ~80 eV, just as Mike has indicated (cf. figs. 4 and A.)